WORLD CONFERENCE ON TIMBER ENGINEERING 2025
BRISBANE, AUSTRALIA
Advancing Timber for the Future Built Environment

CREEP BEHAVIOR OF CROSS-LAMINATED TIMBER-CONCRETE COMPOSITE FLOOR SYSTEM ON FIXED END CONDITION

Kentaro Hatachi[1], Wataru Nishimiya[2], Takuro Mori[3], Yasuhiro Araki[4], Masanobu Sakashita[5], Shoichi Nakashima[6], Hiroshi Isoda[7]

ABSTRACT: Many studies have been conducted on timber-concrete composite systems (TCC) as a new technology for medium to large scale buildings using wood materials. This study focuses on CLT-reinforced concrete composite floors and aims to understand the long-term performance of TCC floors under fixed end support conditions through the bending creep tests. As the results of the bending creep test, the creep coefficient calculated using the power law is about 4, which is about four times smaller than the creep coefficient of concrete slab. In the both-ends fixed condition, it was shown different force condition compare the simply supported condition examined in prior studies, the top surface of the edge of the composite floor bears the tensile force, so that both the concrete and wood sections bear the tensile and compressive forces. Accordingly, the bending stiffness of the floor system was calculated using the formula proposed by FPInnovations based on the γ method, and a larger value was calculated than the experimental value. It was considered this difference due to cracking caused by the concrete bearing tensile forces and the consequent reduction in anchorage, so to understand the long-term behavior of this system is planned to investigate a cracking etc. in detail.

KEYWORDS: Cross-laminated timber, Timber- reinforced concrete composite, Floor, Creep behavior

1 INTRODUCTION

In recent years, there has been an increase in the use of timber in mid- and high-rise buildings due to a combination of environmental concerns and other factors. This development has led to the creation of high-strength and high-rigidity structural materials using timber, such as composite floors. These floors consist of a concrete upper layer and a timber lower layer, with the aim of enhancing rigidity in a rational manner by utilizing the strength characteristics of each component. In this configuration, the concrete is responsible for the compressive forces, while the timber provides resistance to tensile forces in the vertical downward direction. Examples of practical use include 'Te Ara Hihiko' worldwide but are limited to 'PARK WOOD TAKAMORI' and others in Japan. As demonstrated by Ali Tighnavard Balasbaneh et al. [1], the integration of concrete and wood has been shown to reduce environmental impact. In addition, Osama A.B. Hassan et al. [2] have proposed that composite floors can be utilized to decrease the weight of a structure. These factors are expected to drive the development of composite floors in the future, and studies are currently being reported by Guilherme dos Santos Silva et al. [3], Hamidreza Chaboki [4], Eetu Salo [5], and others. Most of these studies are experimental and analytical investigations of the strength and stiffness of floors under simply supported conditions. For instance, the study by Ohki et al. [6] evaluated the shear performance of composite floor slab joints by shear keys. Additionally, Mori et al. [7] conducted creep experiments on composite floors with full-size span composite floor under simply supported conditions to determine long-term performance, and comprehensively examined methods for calculating stiffness, even

[1] Kentaro Hatachi, Graduate School of Advanced Science and Engineering, Hiroshima University, Hiroshima, Japan, m245662@hiroshima-u.ac.jp

[2] Wataru Nishimiya, Former graduate student, Hiroshima Univ., Hiroshima, Japan, wnishimiya@gmail.com

[3] Takuro Mori, Graduate School of Advanced Science and Engineering, Hiroshima University, Hiroshima, Japan, moritaku@hiroshima-u.ac.jp

[4] Yasuhiro Araki, National Institute for Land and Infrastructure Management, Tsukuba, Japan, araki-y92ev@mlit.go.jp

[5] Masanobu Sakashita, Building Research Institute, Tsukuba, Japan, m-saka@kenken.go.jp

[6] Shoichi Nakashima, Building Research Institute, Tsukuba, Japan, nakas@kenken.go.jp

[7] Hiroshi Isoda, Research Institute for Sustainable Humanosphere, Kyoto University, Kyoto, Japan, hisoda@rish.kyoto-u.ac.jp

https://doi.org/10.52202/080513-0436

proposing calculation formulas. However, under the assumption that the composite floor is utilized in a mid-rise building, a segment of the upper portion of the composite floor may potentially bear tensile forces, stemming from the concrete frame and the inflection points situated at the periphery of the slab constituting the continuous floor. Moreover, these tensile forces may result in the formation of cracks in the concrete, leading to a loss of cross-sectional integrity and an increase in deflection due to rotation. There are no research results available for performance evaluation under such more realistic conditions. The objective of this study is to ascertain the long-term performance of TCC floors in the fixed end support condition. To this end, bending creep tests are performed on a 6-meter span floor under uncontrolled air conditions. Additionally, creep and bending tests are conducted on a TCC floor under cantilevering conditions to examine the behavior of the fixed end in greater detail.

2 MATERIALS AND METHODS

There were three test specimens, one fixed at both ends and two cantilevered (Table 1, Fig. 1). The 90-mm-thick reinforced concrete (RC) slab with deformed steel bars in the center of the cross section was utilized. The wood section was cross-laminated timber (CLT), with a thickness of 150 mm and a strength class of Mx60-5-5 as specified by the Japanese Agricultural Standard (JAS). CLT was made 6 mm slits to insert the shear key (Fig.2), which was fixed with adhesive (epoxy resin). As a support condition, the RC slab was cast concurrently with the top of the stub, resulting in its integration, and the CLT was placed merely on the corbels that appeared to protrude from the stub. Table 2 presents the material properties of the specimens. The compressive strength of the concrete for both fixed ends specimen and cantilever specimen 1 was 34.7 N/mm^2 at the time of loading (49 days after placement), 31.1 N/mm^2 at 6 months (243 days) after loading, and 32.9 N/mm^2 at 14 months (434 days) after loading, with no strength increase observed as the material ages. In cantilever specimen 2, the value was 26.7 N/mm^2 at loading (22 days after placement). The both fixed ends specimen was subjected to four-point bending creep testing, while the cantilever test constituted a creep test with concentrated loading. The both fixed ends specimen had a dead weight of 15.5 kN and a loading capacity of 11.4 kN (2.0 kN/m^2), which is the structural design value of the main beam, column, or foundation (1.3 kN/m^2) plus the fixed load (0.7 kN/m^2). The cantilever specimens had a dead weight of 4.7 kN. The load is given in Table 1, and it was modified after the commencement of the test and is detailed in Sections 3.2 and 3.3. The specimen was situated indoors without temperature and humidity control. Each measurement point (Fig.3) was recorded at one-hour intervals, and temperature and humidity meters located near the specimens were also measured at one-hour intervals.

Table 1.

support condition		load [kN]
fixed both ends		11.4 kN (2.0 kN/m^2)
cantilever	1	3.4 kN (2.0 kN/m^2)
	2	10.26 kN (6.0 kN/m^2)

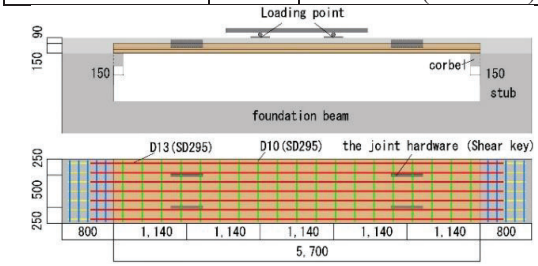

Both fixed ends specimen

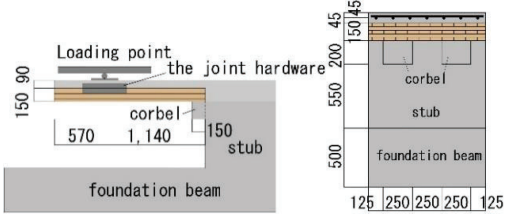

Cantilever specimen support section

Fig. 1. Test specimens [mm]

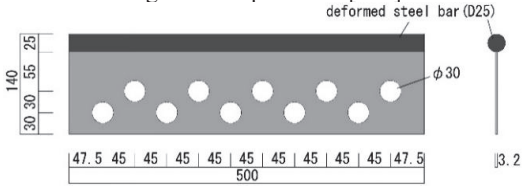

Fig. 2. Joint hardware (Shear key) [mm]

Table 2. Material properties

Wooden part	Tree species: Japanese Ceder CLT (JAS:Mx60-5-5) Bending elastic modulus: 5.97kN/mm^2 Elastic shear modulus: 0.25kN/mm^2 Compressive strength: 24.3N/mm^2 Tensile strength: 15.6N/mm^2
RC slab	Axial reinforcement: 7-D13(SD295) Perpendicular reinforcement: D10@300(SD295)
Joint hardware	Steel plate: 500*115*3.2mm (SS400) Reinforcing bar: D25 (SD295)

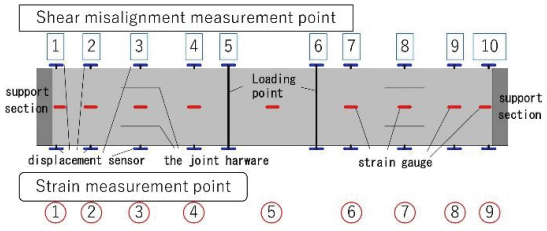

Fig. 3. Measurement locations

https://doi.org/10.52202/080513-0436

3 RESULT

3.1 BOTH FIXED ENDS SPECIMEN

As shown in Fig. 4, the central deflection exhibited a time-dependent change, with the deflection, temperature, and humidity measured at 12:00 on each day. The initial deflection immediately after loading was 4.23 mm, and deflection progressed to 11.47 mm at 707 days after loading. The progression of deflection decelerated at approximately 150 days after loading and remained nearly constant after about 200 days. After approximately 350 days after loading, when the temperature and humidity exhibited an increase during the summer season, the deflection exhibited a renewed increase, though not as much as in the initial period. Subsequently, after approximately 600 days, when the temperature and humidity decreased during the winter season, the deflection ceased its increase and initiated a decrease. Consequently, the seasonal variation in creep deflection, as observed in previous studies [7], was also discerned in this experiment.

Figs. 5, 6 illustrate the cracking behavior of the RC slab, as observed on the loading date, 6 months after loading, and 19 months after loading, respectively. On the loading date, one crack line across the width was observed on the top surface of the RC slab near each support, and the crack lines also extended to the sides. 6 months after loading, two additional cracks were observed on the top surface of the slab at each support. These cracks were mainly located

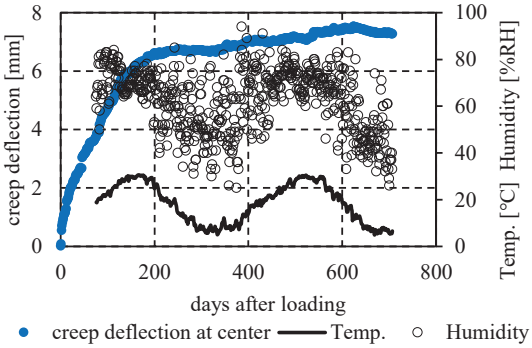

Fig. 4. Change over time of both fixed ends specimen

in areas expected to bear tensile forces, such as the top of the fixed ends and are assumed to affect the measured deflection values by causing cross-sectional defects and rotation. This is examined in detail in Chapter 4. The cracks observed 19 months after loading included some that had progressed from cracks that had been observed up until then, and others that had newly occurred. However, since small cracks had occurred evenly throughout the entire slab, and some were only seen on one side of the specimen, it is suggested that they were caused by the drying shrinkage of the concrete and did not significantly affect the measured deflection values.

The Power law [8] and the calculation method based on the notification of the Ministry of Construction [9] (henceforth referred to as the Notification method) are frequently utilized in Japan to predict creep deflection after 50 years and to calculate the creep coefficient for

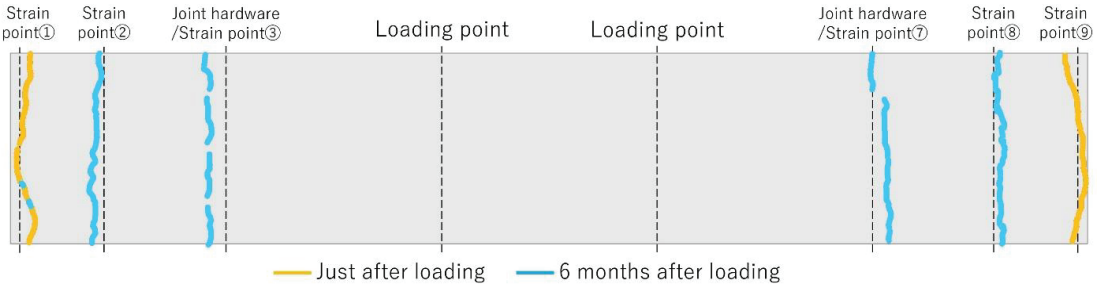

Fig. 5. Cracking behavior of both fixed ends specimen from the top

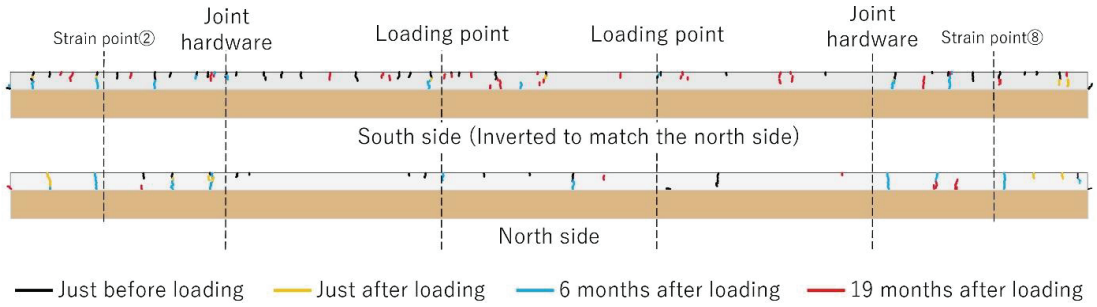

Fig. 6. Cracking behavior of both fixed ends specimen from the side

https://doi.org/10.52202/080513-0436

design purposes. Figs. 7, 8 and Table 3 present the creep coefficient calculated by each method based on the results of the center deflection over time. The All Power law and the All Notification method are calculated using all data post-loading, while the Secondary Power law and Secondary Notification method are calculated using data after 200 days (secondary creep period) post-loading. The average creep coefficient using all the data is 5.9. The creep coefficient for the data after 200 days is 3.6 and has been observed to gradually increase as the data accumulates; however, it is expected to decrease slightly more depending on the rate of decrease in summer variability in the coming year. Therefore, it is considered that the deflection after 50 years will be less than four times the initial deflection.

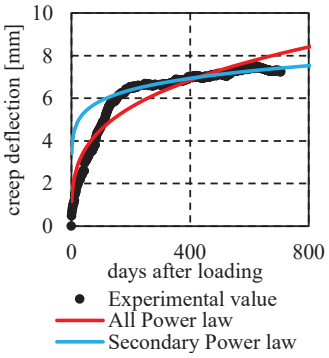

	All	SR
a	0.30	0.12
b	0.06	0.53
A	1.16	3.42
N	0.30	0.12
c	0.27	0.81

Fig. 7. Calculation by the Power low

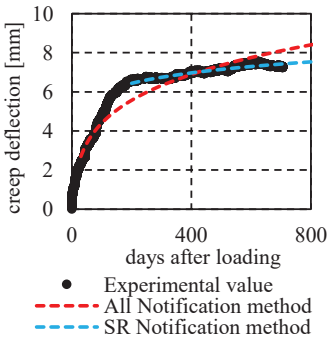

	All	SR
c	-0.20	-0.07
d	0.64	0.02
K	0.19	0.29

Fig. 8. Calculation by the Notification method

Table 3. Calculation results of the creep coefficient

data	All	Secondary
the Power Law	6.02	3.57
the Notification Method	5.38	3.51

3.2 CANTILEVER SPECIMEN 1

3.2-1 CREEP TEST

The load for this test was 3.4 kN (2.0 kN/m^2), which was consistent with the both fixed ends specimen. Fig. 9 shows the deflection was measured over time, with the measurements of deflection, temperature, and humidity being recorded at 12:00 daily. Following the initial deflection in the loading direction at the onset of the loading process, the deflection progressed in the opposite direction to the loading. In the creep experiment (Naga, et al., [10]), using a cantilever RC slab cast in half-precast material, the test specimen, which was in the process of creep deflection, exhibited constant or slight recovery behavior when the temperature was high. This experiment also commenced on March 9, when the temperature began to rise, which is the time when warping is most likely to be observed. The deflection of the specimens exhibited a pattern of increase and decrease after approximately 120 days following the application of loading, which may be attributable to the influence of temperature and humidity. Specifically, between approximately 120 and 150 days after loading, deflection increased in proportion to increasing humidity. However, after 150 days, deflection decreased in proportion to decreasing humidity, thereby confirming the significant effect of temperature and humidity. Fig. 10 shows the change over time of the strain in the center of the specimen in the direction orthogonal to the specimen axis. The strains of the rebar at each measurement point indicate the compression side, thereby confirming that the lower side of the specimen bears tensile force, while the upper side of the specimen bears

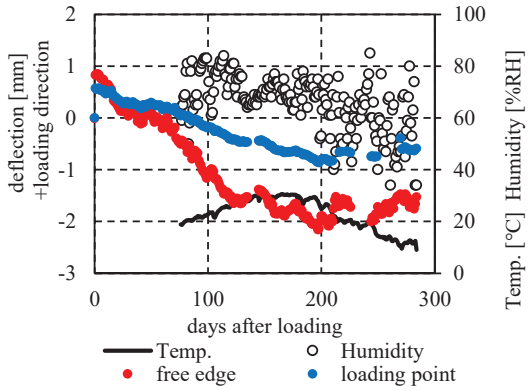

Fig. 9. Change over time of cantilever specimen 1

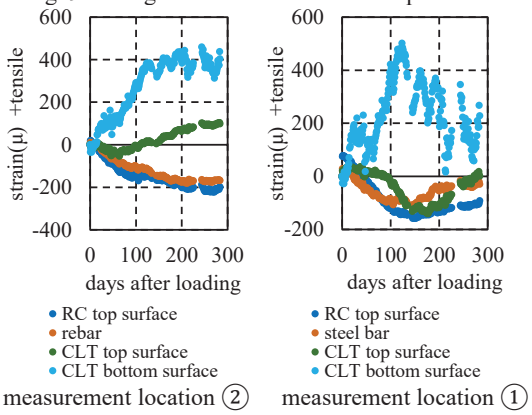

measurement location ② measurement location ①

Fig. 10. Change over time of strain

https://doi.org/10.52202/080513-0436

compressive force as it warps. Additionally, it was observed that the strain on the underside of the CLT exhibited fluctuations during periods of significant humidity variations, a phenomenon that was accompanied by changes in deflection. Fig. 11 illustrates the cracks observed in the specimen. The cracks exhibited a lesser increase due to warping in a direction opposite the applied loading.

3.2-2 BENDING TEST

From the results of Section 3.2-1, it was determined that the magnitude of the applied load was inadequate to induce long-term displacement. Consequently, the creep test was terminated, and the specimens were unloaded. Subsequently, monotonic loading tests were conducted on the specimens to ascertain the ultimate performance of the composite floor. Fig. 12 shows the load-displacement relationship and Fig. 13 is an expanded version extending up to a load of 15 kN. The initiation of the first crack was observed on the top surface of the specimen at a load of 9.4 kN and a displacement of 1.14 mm at the loading point. Subsequently, the slab steel bars yielded in tension at approximately 58 kN, and the load continued to increase slightly, reaching a maximum load of 68.5 kN at a displacement angle of 6%, which was the limit of the displacement transducer's measurement, thus terminating the test. Fig. 14 shows the fracture properties. The specimen exhibited cracks that penetrated the RC portion in the width direction, with a total of five locations observed on the top surface. The width of these cracks ranged from 6.00 mm near the support area to a minimum at the specimen's edge. At the support, the CLT exerted an upward force on the RC, with the corner of the corbel serving as the center of rotation, thereby progressing the failure. This resulted in a compressive force on the bottom surface of the CLT near the support, leading to cracking observed at the boundary between the orthogonal and parallel layers on the underside of the CLT. As a result, 3.4 kN that the load carrying in this creep test was understood insufficient load value to make a crack. Consequently, to conduct an additional creep test under the cantilever condition, it is necessary to apply a loading load of at least 9.4 kN.

3.3 CANTILEVER SPECIMEN 2

In accordance with the findings outlined in Section 3.2, this system floor's creep test under cantilevered conditions was reinitiated by making a new specimen. The specimen's outline is delineated in Section 2. At the initiation of loading, the shoring was removed at loading loads of 2, 3, 4, 5, and 6 kN/m^2 to assess deflection and the presence of cracks on the top surface of the specimen. At a load of 10.26 kN (6.0 kN/m^2), a crack occurred at the top of the specimen at approximately 50 mm from the anchorage edge (Fig. 15). The width of this crack was approximately 0.05 mm. Fig. 16 illustrates the temporal progression of the deflection at the loading point and at the specimen's

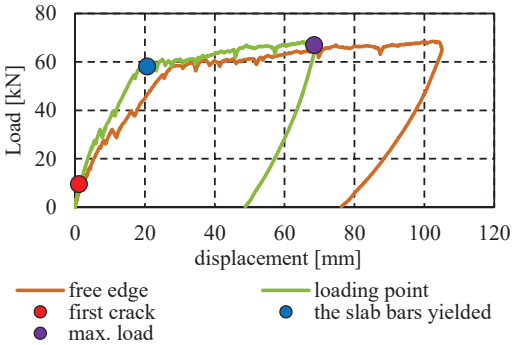

Fig. 12. Load-displacement relationship

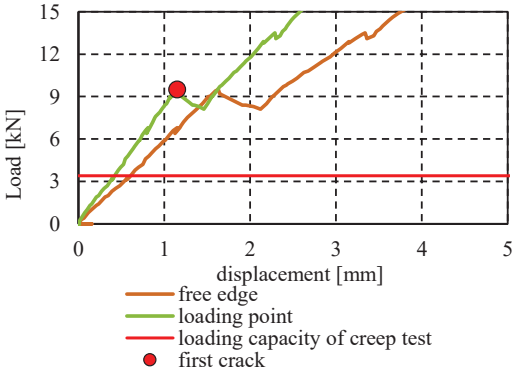

Fig. 13. Zoom up Fig.12

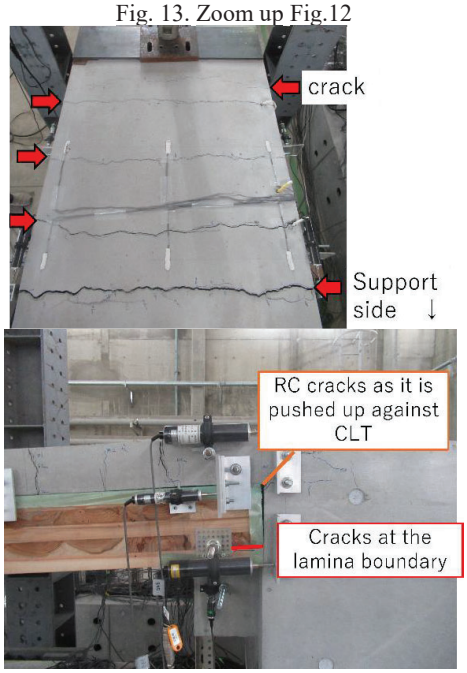

Fig. 14. Filure mode of bending test

https://doi.org/10.52202/080513-0436

extremity, extending up to 227 days following the application of the load. That shows the deflection, temperature and humidity measurements obtained at 12:00 daily. The initial deflection at the loading point was recorded as 1.5 mm, and it underwent a progression to 2.5 mm within the span of 227 days following the application of the load. The rate of increase in deflection after the initial deflection is not as large as for the both fixed ends specimen.

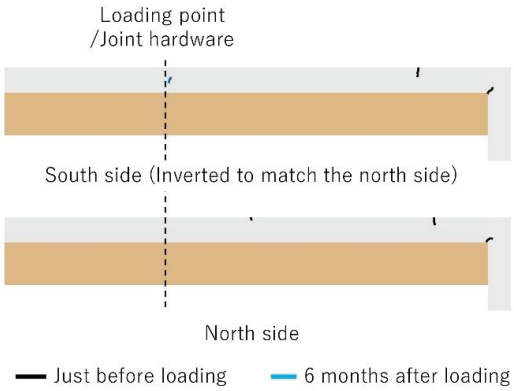

Fig. 11. Cracking behavior of cantilever specimen 1 from the side

4 STIFFNESS REDUCTION DUE TO CRACKS

This chapter reports on the stiffness reduction due to cracking that occurred in the early test stages for each specimen.

4.1 BOTH FIXED ENDS SPECIMEN

As illustrated in Fig. 17, the deflection variation of the both fixed ends specimen during loading is demonstrated. Figs. 18, 19 present the strain measurement locations (1) and (9), respectively. The load was applied by removing the support with the weight on it. Upon removal of the support and stabilization of the specimen (initial deflection), it was observed that the rebar within the RC slab were in a state of tension, while the upper surface of CLT was in a state of tension and the lower surface of the CLT was in a state of compression. This observation indicates that cracking occurred on the top surface of the RC slab in proximity to the measurement location, with the cracks subsequently propagating into the interior. Additionally, it was observed that the deflection increased concurrently, suggesting that the cracks induced rotation and deflection of the floor. The precise extent of the deflection increase necessitates further examination; however, it is estimated to be approximately 1.00 mm, as

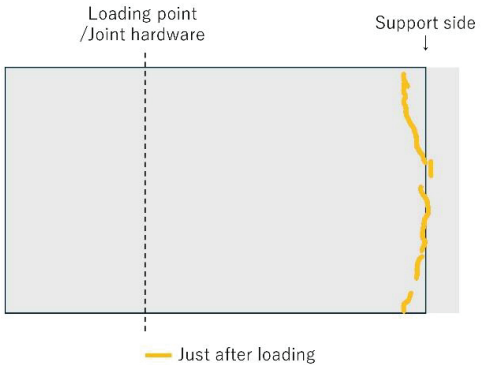

Fig. 15. Cracking behavior of cantilever specimen 2 from the top

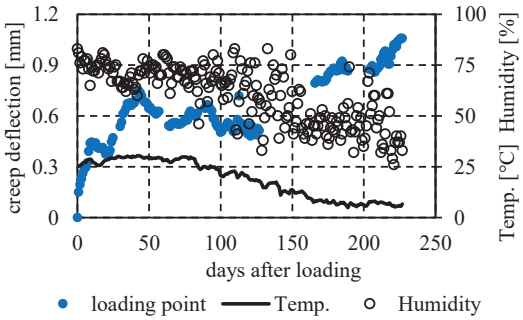

Fig. 16. Change over time of cantilever specimen 2

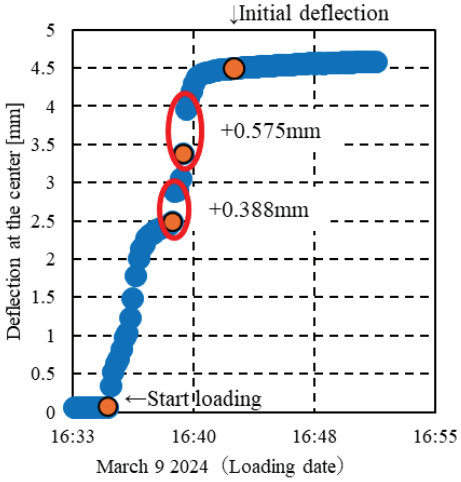

Fig. 17. Deflection behavior to initial deflection of both fixed ends specimen

determined through visual inspection (highlighted in red in Fig. 17).

The presence of cracks in the RC slab and CLT leads to the deflection of their edges, as illustrated in Fig. 20. This deflection can be similar to that observed in the simply supported condition depicted in Fig. 21. The width of the cracks, measured immediately after loading, was found to be an average of 0.3 mm. Utilizing this measurement, the

https://doi.org/10.52202/080513-0436

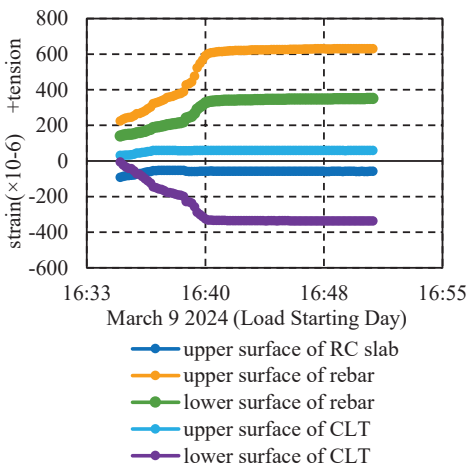

Fig. 18. Strain measurement location ① to initial deflection of both fixed ends specimen

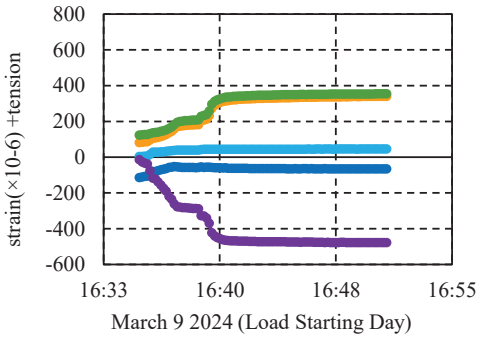

The counterexample is the same as Fig. 18.

Fig. 19. Strain measurement location ⑨ to initial deflection of both fixed ends specimen

rotation angle θ was calculated, as depicted in the figures. Furthermore, the central deflection in the simply supported condition was determined to be 6.23 mm, as calculated using Eq. (1).

$$v\left(\frac{L}{2}\right) = \frac{59}{180} \cdot L \cdot \theta(0) \quad (1)$$

$$= \frac{59PL^3}{1500EI} \quad (2)$$

Where,

$v\left(\frac{L}{2}\right)$	: deflection at central point	[mm]
L	: span	[mm]
$\theta(0)$	: angle of rotation	[N]
P	: loading capacity	[N]
EI	: bending stiffness	[kN·mm^2]

This is the incremental deflection contributed by the rotation caused by the cracks. However, in Fig. 20, the restraint of the CLT edge by the RC slab is ignored. Therefore, we consider the deflection schematically shown in Fig. 22 to be a more realistic form, in which the floor is under conditions similar to those of fixed support at both ends (Fig. 23). The ratio of Eq. (2) and (3) was used to calculate the central deflection for the fixed end support condition, which was determined to be 1.36 mm. This value is larger than the deflection increases due to cracks (approximately 1.00 mm), as determined by visual estimation (Fig. 17).

$$v\left(\frac{L}{2}\right) = \frac{PL^3}{125EI} \quad (3)$$

It is assumed in Figs. 20, 22 that the cracks have advanced to a depth that cuts through the cross-section of the RC slab, but it is highly likely that the cracks did not reach the bottom edge of the slab immediately after loading. To determine the cause of the difference between the calculated and visually determined values, it is necessary to closely examine the crack depth as well as other concrete behaviors so that the amount of deflection increase can be more accurately calculated.

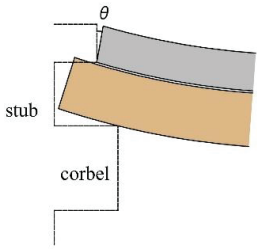

Fig. 20. Schematic diagram1

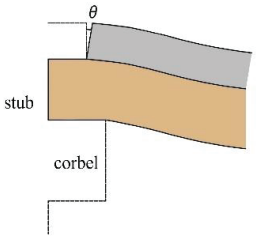

Fig. 22. Schematic diagram3

Fig. 21. Schematic diagram2

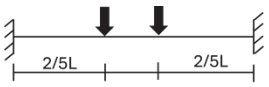

Fig. 23. Schematic diagram4

4.2 CANTILEVER SPECIMEN

The reduction in stiffness due to cracking in cantilevered specimen 2 was considered. Fig. 24 shows the deflection at the loading point at loads of 2~6 kN/m^2. The specimen was considered as a cantilever beam with the loading load as the concentrated load and the weight of RC slab and CLT as the distributed load, as shown in Fig.25. The bending stiffness was calculated using the load and deflection differences at loads of 2 and 5 kN/m^2, employing Eq. (4) to yield a result of 8.73×10^9 [kN·mm^2].

https://doi.org/10.52202/080513-0436

However, when the bending stiffness was calculated from the deflection at a load of 6 kN/m^2, it was 4.55×10^9 [kN·mm^2], which was approximately one-half that before cracking.

$$EI = \frac{a^2}{24\delta_e}(8Pa + 6wL^2 - 4wLa + wa^2) \qquad (4)$$

Where,

a	: span to loading point	[mm]
δ_e	: deflection	[mm]
w	: distributed load	[N/mm]

This is due to the loss of cross-section of the RC slab due to cracking, and the increase in deflection due to rotation, resulting in a decrease in apparent stiffness.

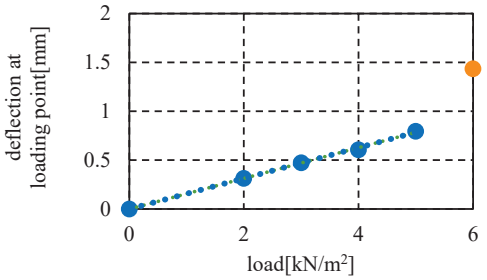

Fig. 24. Initial load-deflection relationship of cantilever specimen 2

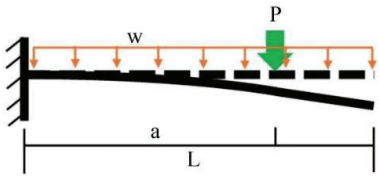

Fig. 25. Schematic diagram of cantilever specimen

Here, Nishimiya et al. [11] calculated the stiffness of a cantilevered specimen using the bending stiffness formula [12] for composite structures under fixed end conditions, which was proposed based on the γ method [13], a stiffness calculation formula for composite beams. The bending stiffness was calculated to be 3.01×10^9 [kN·mm^2], which is 0.66 times greater than the stiffness calculated from the initial behavior (after cracking) of this experiment. In Equation [12], the concrete is ignored and the reinforcement bears the tensile force due to the moment, but the cracks in the initial stage of this experiment were not deep enough to penetrate the concrete section, which may be the cause of this difference.

5 CONCLUSIONS

The purpose of this study is to understand the long-term performance of TCC floors in fixed end support conditions. Bending creep tests were performed on a floor with a span of approximately 6 m. Creep and bending tests were also performed on a TCC floor in cantilevered condition to investigate the behavior of the fixed ends in more detail.

1. In the creep test of the specimens fixed at both ends, the initial deflection at the center was 4.2 mm, but it progressed to 11.5 mm in 707 days after loading. The creep coefficient was about 5.9 for all data and about 3.6 for the secondary creep period data. And seasonal variations in creep deflection were observed.

2. Since the loading of the cantilever specimen was found to be insufficient in the initial creep test, a monotonic loading test was conducted to confirm the load at which cracking would occur. As a result, a new cantilever specimen was installed, the load was increased, and the creep test was restarted. While the initial deflection at the loading point was 1.5 mm, it progressed to 2.5 mm in 227 days after loading.

3. From the experimental results, it was confirmed that the stiffness of each specimen decreased before and after cracking, and specific calculation methods were investigated regarding the effects of cracking.

In the future, we will propose a formula for calculating the stiffness of composite floors. This formula will be based on further confirmation of the effect of cracking on stiffness. After this, a methodology will be established for the estimation of long-term deflection. Thus, these creep specimens will continue to be investigated.

ACKNOWLEDGEMENTS

The authors acknowledge the funding received from Public/Private R&D Investment Strategic Expansion PrograM (PRISM) and Programs for Bridging the gap between R&D and the IDeal society (society 5.0) and Generating Economic and social value (BRiDGE).

REFERENCES

[1] Ali Tighnavard Balasbaneh, et al.: LCA & LCC analysis of hybrid glued laminated Timber–Concrete composite floor slab system, Journal of Building Engineering, 49, 104005, 2022

[2] Osama A.B. Hassan, et al.: Cross-laminated timber flooring and concrete slab flooring: A comparative study of structural design, economic and environmental consequences, Journal of Building Engineering, 26, 100881, 2019

[3] Guilherme dos Santos Silva, et al.: Proposed correction to the Gamma method for estimating the bending stiffness of CLT panels, Structures, 68, 107214, 2024

[4] Hamidreza Chaboki: A CONNECTION FOR TWO-WAY SPANNING CROSS-LAMINATED TIMBERCONCRETE COMPOSITE FLOORS, master's thesis, UNIVERSITY OF NORTHERN BRITISH COLUMBIA, 2024.4

[5] Eetu Salo: Comparing the classical elastic theory of layered beams to the Gamma and the Timoshenko methods for cross-laminated timber-concrete composite slabs, master's thesis, Aalto University, 2024

[6] Fumiaki OHKI: Study on composite slabs of Cross Laminated TimberReinforced Concrete with mechanical joint, Doctor's thesis, Nihon University, 2021.3

[7] Takuro Mori, et al.: Experimental long-term behavior of a CLT-concrete composite floor system connected with steel plate, Constructuon and Building Materials, 466, 140096, 2025

[8] Japan Housing and Wood Technology Center: Strength Test Manual of Structural Timber, pp.49-58, 2011

[9] MC normative notice, 1446, 2000

[10] Ryotaro NAGA, et al.: Long-term loading tests of cantilevered reinforced concrete slabs with half precast elements, Proceedings of the Japan Concrete Institute, 45, 2, pp.553-558, 2023

[11] Wataru Nishimiya, et al.: Study on Long-Term Performance of CLT-RC Composite Floors under Fixed-Edge Support Conditions, Part 2: Study on the Passage up to 284 Days after Loading and Calculation of Stiffness Using the γ-Method, Research Reports of AIJ, Chugoku Branch, 47, pp.140-143, 2024

[12] Samuel Cuerrier-Auclair, FP Innovations: Design Guide for Timber-Concrete Composite Floors in Canada, 2020

[13] EN 1995-1-1: Eurocode 5: Design of timber structures - Part 1-1:General – Common rules and rules for buildings, Annex B (Informative): Mechanically jointed beams, pp.110-113, 2004

https://doi.org/10.52202/080513-0436